

Tracking multiple fluorescent particles in two dimensions in a confocal microscope

Zhaolong Shen and Sean B. Andersson

Department of Mechanical Engineering, Boston University, Boston, MA 02215
{zlshen,sanderss}@bu.edu

Abstract—In this paper, we describe a system for tracking multiple fluorescent particles in a confocal microscope. The tracking algorithm relies on position estimates derived from fluorescence measurements taken at a small number of discrete locations combined with an LQG controller. We report experimental results of tracking a single fixed particle, a single diffusing particle, and two fixed particles.

I. INTRODUCTION

Within the past few years, tracking of fluorescent particles in liquid environments has been used widely by biologists to study molecular dynamics at submicron resolution, greatly exceeding the resolution limits of classical optical microscopy. Recent applications include the study of the nuclear trafficking process of influenza virus infection by tracking single vRNPs in living cells in real time [1], an exploration of the mechanisms leading to slow diffusion rates in cell membranes [2], and the mechanism of the signal transduction mediated by the G-protein-coupled receptors [3]. In addition to such single particle tracking applications, researchers have also tracked multiple particles simultaneously, with applications including the measurement of heterogeneities in the microenvironment [4], [5] and micromechanical properties [6]. Furthermore, such methods can even be used for drug and gene delivery [7].

Unfortunately, most tracking methods mentioned above rely on the use of a wide-field fluorescent image captured by a CCD camera. This scheme is essentially limited to tracking particles moving in or near the focal plane. Its spatial and temporal resolutions are determined by the characteristics of the camera and the details of the position estimation algorithm used. To estimate the position of a fluorescent particle in three dimensions, one must either obtain images at different axial positions or take advantage of defocusing to get information about the position along the optical axis [8], [9]. Either scheme leads to a reduction in the temporal resolution.

To overcome such limitations, several alternative approaches have been developed to track a single particle moving in the plane. These schemes rely on point detectors in a single or multi-photon microscope. One of the early approaches proposed rapidly steering the laser focus around a circle and estimating the particle position from collected fluorescence intensity fluctuations [10]. This basic scheme has been used in a variety of recent efforts. In [11], a feedback controller was introduced to steer the center of the scanned circle. To track in three dimensions, the focus

was circularly scanned in two different axial planes in a sequential fashion [12], or a pair of laser beams were focused at different axial positions [13]. This latter scheme has been quite successful and has tracked quantum dots diffusing with coefficient as high as $20 \mu\text{m}^2/\text{s}$. Other tracking approaches include [14]–[16], which track particles moving in three dimensions without scanning the focus but at expense of a more complicated detection system. Recent reviews of the state-of-the-art can be found in [17]–[19].

Our tracking system is composed of a confocal microscope with a piezoactuated nanopositioning stage, a microcontroller and tracking algorithm based on the use of a linear quadratic Gaussian controller. In this work, we use a position estimation algorithm introduced by one of the authors [20], [21], to estimate the particle position by taking measurements of the fluorescence intensity at several discrete locations. The overall implementation is simpler in terms of the experimental apparatus than existing methods and extends naturally to the tracking of multiple particles. It is also important to note that all tracking results reported to date for particles with diffusion coefficients above $0.1 \mu\text{m}^2/\text{s}$, including those presented here, utilize quantum dots and consequently operate with high signal-to-noise ratio (SNR). The estimation algorithm at the core of our method has been shown to be effective at low SNR [21] and thus we expect our algorithm to maintain performance in noisier settings such as those involving fluorescent dyes inside live cells.

II. ALGORITHM DESCRIPTION

In this section we provide an overview of our tracking algorithm. It was originally introduced in [22] and details can be found there. Our system, shown in Fig. 1, consists of a confocal apparatus and a 3-D translation stage used to move the sample relative to the detection volume of the microscope.

We develop a linear stochastic model of the system by first describing the evolution of each particle to be tracked as a random walk:

$$x_i[k+1] = x_i[k] + \sqrt{2D_i\Delta t}w[k], \quad i = 1, \dots, N_p \quad (1)$$

where $x_i[k] \in \mathbb{R}^2$ is the position of the i^{th} particle at time step k , Δt is the control sampling period, D_i is the diffusion coefficient of the i^{th} particle, $w[\cdot]$ is a zero mean, unity variance Gaussian white noise process, and N_p is the number of particles to be tracked. To this we append the transfer function of the translation stage. We assume we

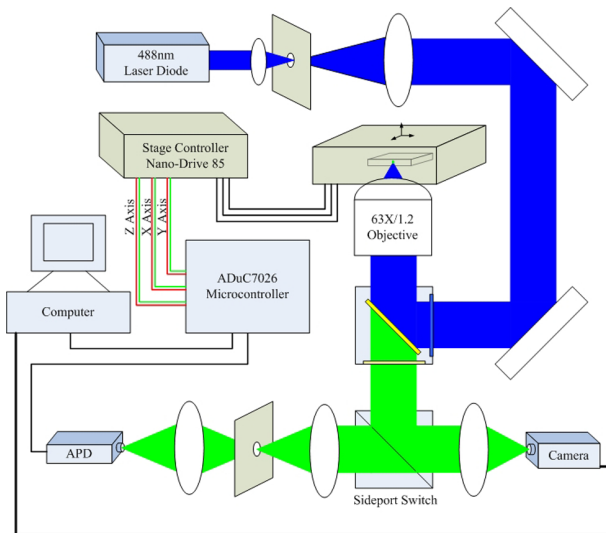


Fig. 1. System schematic for the tracing system. The excitation source (blue) is focused through the objective lens onto the sample. The emitted signal (green) is separated from the excitation using a dichroic mirror and then focused either onto a CCD or through a pinhole onto an avalanche photodiode. Motion of the stage is achieved using a three-axis piezostage. System control is performed using a microcontroller.

have perfect measurements of the position of the stage and noisy measurements of the position of the particles with respect to a fixed frame. Then, tracking of a single particle is achieved through the use of a linear quadratic Gaussian (LQG) controller where the cost function is given by

$$J = \sum_{k=1}^{\infty} (\lambda_e e(k)^2 + \lambda_u u^2) \quad (2)$$

where e is the tracking error, defined as the difference between the stage position and the particle, and u is the highest derivative of the driving voltage of the piezostage. We note that the actual control signal for the stage is part of the system state. For multiple particles, an LQG controller is designed for each independently and the system simply alternates between them in a cyclic fashion.

The position of a particle cannot be measured directly but must be inferred from the measurements of the fluorescence intensity. The fluoroBancroft algorithm, introduced in [20], [21], provides an analytical solution to the localization problem from a collection of as few as three measurements taken at three non-colinear points. A measurement of the fluorescence intensity at a point (x, y) can be related to the position of the point source (x_o, y_o) through the point spread function (PSF), approximated by

$$I(x, y) = me^{-\frac{(x-x_o)^2 + (y-y_o)^2}{2w_o}} + \eta_B + \eta_S \quad (3)$$

where w_o is the width of the PSF, η_B is the background fluorescence, and η_S represents the shot noise. The intensity measurement is converted into an estimate of the range to the source. The fluoroBancroft algorithm expresses a collection of such measurements as an overdetermined linear system that is then solved using a Moore-Penrose generalized inverse.

In our tracking algorithm the stage is moved through a sequence of measurement positions at each time step k . These points are arranged on a circle centered on the current position of the stage designated by the LQG controller. The measurements are used to estimate the position of the particle. That estimate is then taken to be the system measurement of the particle position, allowing the LQG controller to be updated.

III. IMPLEMENTATION

The tracking scheme was implemented on a custom confocal microscope (see Fig. 1). A 488 nm laser (ChromaLASE, Blue Sky Research, CA, USA) was used for excitation. The beam was expanded to fill the back aperture of the objective lens (water immersion, 63x, 1.2 N.A. C-Apochromat, Carl Zeiss, NY, USA) and spatially filtered using a $5 \mu\text{m}$ pinhole. The beam was directed into the objective lens using a dichroic filter (T495LP, Chroma, VT, USA). The resulting fluorescence was collected by the same objective lens, passed through the dichroic filter and a bandpass filter (HQ625/30m, Chroma, VT, USA), and then focused through a $25 \mu\text{m}$ pinhole and onto an avalanche photodiode (APD) (SPCM-AQR-14, Perkin Elmer, MA, USA).

Motion of the sample was achieved using a three-axis piezoelectric stage (Nano-PDQ, Mad City Labs, WI, USA). The algorithm was implemented on a microcontroller board (ADuC7026, Analog Devices, MA, USA). Control signals from the microcontroller were passed through a power amplifier (Nano-Drive85, Mad City Labs, WI, USA) and then applied to the piezos. The transfer function of the stage was identified. The results have been previously reported [22].

The objective lens was mounted in an inverted optical microscope (Axiovert 200, Carl Zeiss, NY, USA). The collected light could be diverted onto a CCD camera (Retiga EXi, Qimaging, BC, Canada) to produce a wide-field image or to the APD for the confocal measurement.

A user interface was created in Matlab. Through this interface, the system parameters were defined, including the N.A. of the objective lens, the background noise level, the number of particles to be tracked, their diffusion coefficients, the number of measurements to take for each position estimation, the radius of the circle describing the measurement pattern, the integration time for each measurement, the modeled measurement noise arising from the position estimator, the weighting matrices for the LQR controller, and the update rate for the LQG controller. Note that this update rate was constrained to be larger than $N_p N_m \Delta t_I$ where N_p was the number of particles to be tracked, N_m was the number of measurements to collect for each particle at every time step, and Δt_I was the integration time for each measurement.

After selecting the parameter values, the system was initialized using the CCD camera. First, the tracking range of the scanning system was displayed on the CCD image. The sample was then moved using a coarse positioner until a collection of particles was visible within the tracking range. To obtain their initial positions, the user simply clicked on the particles of interest. We note that initialization could

also be performed by other methods such as searching the detection region until a sufficiently high intensity was found or by keeping the detection volume fixed until a sufficiently high signal was detected (indicating a fluorescent particle had diffused into the focal volume). The corresponding pixel coordinates were translated into the lateral coordinates of the piezostage. These initial conditions together with all the parameters were then transferred to the microcontroller using the serial port, the optical signal was diverted to the APD, and the tracking experiment begun. At each time step, the stage was driven around the measurement pattern for each particle in turn. The estimated system state as well as all the fluorescence measurements were recorded and transmitted back to the host system over the serial link.

A diagram of the entire scheme is shown in Fig. 2.

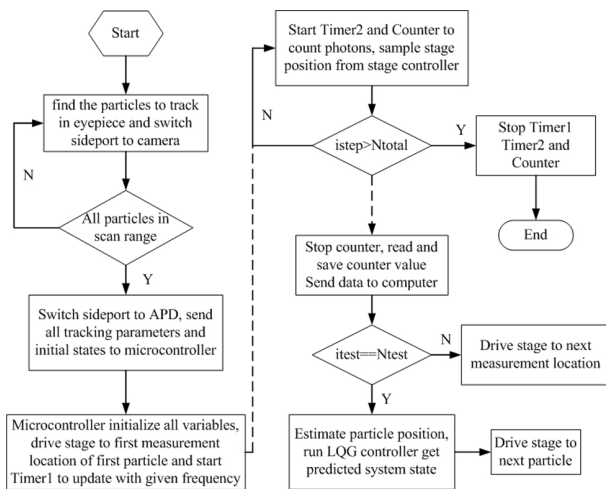


Fig. 2. Flow diagram of our algorithm, from initialization to tracking.

IV. EXPERIMENT SETUP

To test the tracking algorithm, a series of experiments using quantum dots (QD625, Invitrogen, USA) were performed. In all the experiments, a measurement constellation of four points arranged on a circle was used (see Fig. 3). The radius of the circle was set, through trial and error, to 125 nm when tracking a single particle, and to 175 nm when tracking multiple particles. The laser focus was moved counterclockwise through the constellation, starting from the right-most location (denoted location 1), through to the bottom location (location 4). The integration time for each measurement location was set to 2 ms. The background noise rate, estimated by collecting data from a blank sample, was set to 5 counts/ms. The width of the point spread function was set to $w_o = 0.25 \mu\text{m}$. The covariance of the noise in the position estimate was set to $10^{-4} \mu\text{m}^2$ in each axis.

During single particle tracking, the update rate for the position of the stage, and therefore the motion around the sampling points, was set to 20 Hz. The corresponding update rate for the LQG controller was 5 Hz. To keep this 5 Hz rate when tracking two particles, the update rate was increased to 40 Hz. The weights for the LQR cost function were set

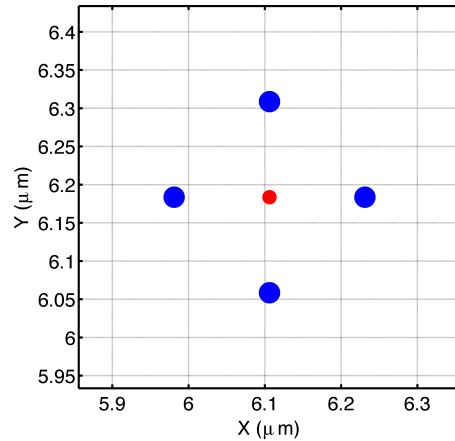


Fig. 3. In this work we use a four-point measurement constellation. The measurement locations are equally spaced around a circle. It is the position of the center of this circle that is controlled using the LQG algorithm.

to $\lambda_e = 1 \times 10^{40}$ and $\lambda_u = 1 \times 10^{-40}$, reflecting that u , the highest derivative of the control signal in the piezostage model, is essentially unrestricted because it is only used by the Kalman filter to get the estimated system state. The actual stage driving voltage is determined from the corresponding component of the predicted system state.

V. EXPERIMENTAL RESULTS

A. Tracking a fixed particle

We first applied the algorithm to track a fixed particle. A solution of quantum dots was dried onto a cover slip. A drop of glycerol was then placed on the cover slip and the cover slip sealed onto a glass slide. The estimated trace of the particle is shown in Fig. 4(a). The initial condition, determined by user click on the CCD image, was approximately 150 nm away from the final average estimated position. The LQG algorithm converged to within 25 nm of this final average position, approximately an order of magnitude better than the diffraction limit of the optical system, within three steps. The final estimate error is better seen from the individual traces of the x and y estimates in Figs. 4(b) and 4(c). The standard deviation in the x signal after the fourth step was 10 nm while the standard deviation in the y signal was 11.5 nm. Since the noise in the position estimate is zero mean, this yields a steady state position error of 15.2 nm, well below the Rayleigh limit. For a fixed bead, the main source of error is the measurement noise, filtered through to the position estimates by the fluoroBancroft algorithm, and to a lesser extent by the modeling errors and quantization errors in the analog-to-digital and digital-to-analog conversion.

The measured fluorescence intensities at the four measurement positions are shown in Fig. 5. The average count per sample period in each signal was greater than 400. This is significantly above the background level of 10 counts in the same sample period, indicating that we are indeed measuring fluorescence from a source particle. The four

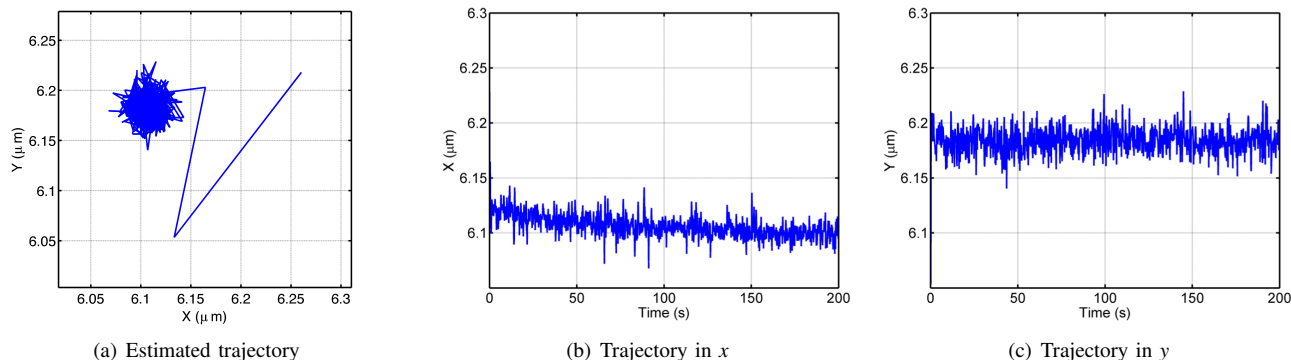


Fig. 4. Tracking a single fixed particle. The trajectory of the focal point converged rapidly to the source particle. The final steady state standard deviations in x and y were 10 nm and 11.5 nm respectively, yielding a steady state position error of 15.2nm.

signals share the same qualitative shape, indicating that the average position of the stage is centered on the particle.

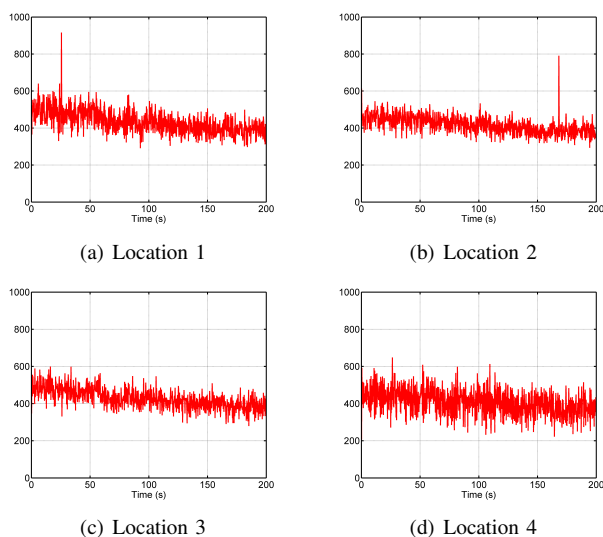


Fig. 5. Photon counts measured at each of the four points of the measurement constellation. The average count per sample period of greater than 400 counts is significantly above the background rate, indicating the presence of a fluorescent particle. In addition, due to the symmetry of the measurement locations, all four signals are qualitatively similar.

B. Tracking a diffusing particle

In these experiments, a solution of quantum dots was prepared in a 90% dilution of glycerol in water, yielding a viscosity of 219 cP [23]. From the Stokes-Einstein relation for the diffusion coefficient of a spherical particle,

$$D = \frac{k_B T}{6\pi\eta a} \quad (4)$$

where k_B is Boltzmann's constant, T is the temperature, η is the viscosity, and a is the radius of the particle, we find $D = 0.1 \mu\text{m}^2/\text{s}$. A small volume of this solution was sealed between a cover slip and a glass slide. The quantum dots were thus free to diffuse in three directions.

Preliminary results suggested that our preparation yielded small collections of bound quantum dots rather than isolated

ones. This would lead to a smaller diffusion coefficient and thus we set $D = 0.1 \times 10^{-4} \mu\text{m}^2/\text{s}$. The remaining parameters were kept unchanged. As before, the system was initialized by clicking on the particle to be tracked in the wide field image.

The results of a tracking run are shown in Fig. 6. The estimated position, shown in Fig. 6(a), clearly illustrates the diffusive nature of the particle motion. The measured photon counts at position one of the measurement constellation are shown in Fig. 6(b). Due to space limitations only the values from this position are shown. As discussed for the single particle case, however, the measurements from the other three positions exhibit the same qualitative behavior and the same signal levels. Note that in this case the photon counts exhibit a slow variation. This reflects the untracked diffusive motion of the particle along the optical axis (out of the plane). As the particle moves away (towards) from the plane, the fluorescence intensity diminishes (increases), yielding the slow fluctuations exhibited. As shown in [21], the position estimator is invariant with respect to the intensity level (assuming the SNR is high enough) and as a result the tracking algorithm is not perturbed by such fluctuations so long as they are slow relative to the controller rate.

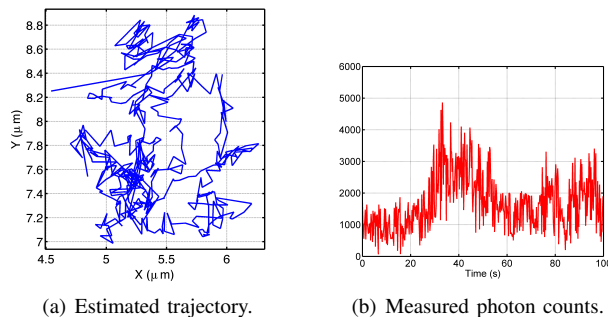


Fig. 6. Tracking a single diffusing quantum dot with $D = 0.1 \mu\text{m}^2/\text{s}$. The first step in the trajectory (from $(x,y) \approx (4.5\mu\text{m}, 8.2\mu\text{m})$) is large due to initialization error. The intensity measurement shown here is from position 1 of the measurement constellation; the others three positions show similar signals. Note that the slow fluctuations in the intensity reflect diffusion of the particle along the optical axis.

While the measured signal level strongly indicates that

the algorithm was tracking a fluorescent particle and not simply responding to background noise, we performed two simple experiments to verify the results. In the first, we initialized the tracking algorithm in a region of pure background. As shown in Fig. 7(b), the measured photon counts are essentially zero. Due to a background threshold in the position estimation algorithm, measured photon counts at the background level do not yield a position update. As a result, at low signal levels the center of the measurement pattern remains fixed. We then switched the fluorescence signal to the CCD camera and, using the coarse positioners on the piezostage, moved a quantum dot near to the focal volume. Finally, the fluorescence signal was switched back to the APD. This switch occurred at time step 610 and, as seen in Fig. 7(b), the fluorescence counts immediately jumped. The tracking algorithm then began following the diffusing particle. The resulting trajectory is shown in Fig. 7(a).

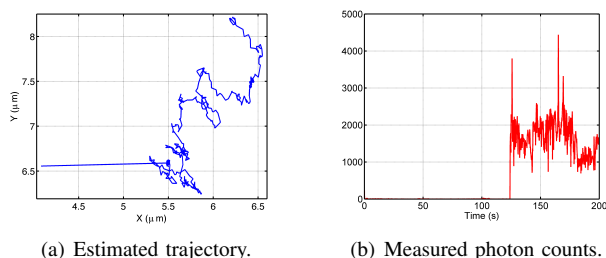


Fig. 7. Capturing a diffusing particle. The system was initialized in a region with no quantum dots. At time step 610, a quantum dot was brought into the focal volume and the tracking algorithm immediately locked on and began following the particle.

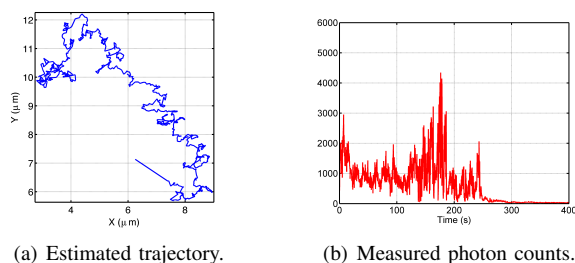


Fig. 8. Losing a diffusing particle. The system was initially tracking a diffusing particle. At time step 1000 the tracking controller was disabled, leading to a slow decline in the measured photon counts. This decay is consistent with the quantum dot diffusing away from the focal volume.

In the second experiment, we initialized the system in the normal fashion but after tracking for a period of time, disabled the tracking controller. The system continued to collect fluorescence measurements but no longer updated the particle position or attempted to follow it. The particle then slowly diffuses away, leading to a gradual decay of the fluorescence intensity to the background level. The particle trajectory is shown in Fig. 8(a) and the measured photon counts at position 1 of the measurement constellation are shown in Fig. 8(b).

C. Tracking two particles

In this experiment we used the preparation of fixed quantum dots and selected a region containing two particles. The initial image is shown in Fig. 9. (The third particle in the upper left corner of the image was not part of the experiment.) We arbitrarily label the lower particle as particle one and the upper particle as particle two.

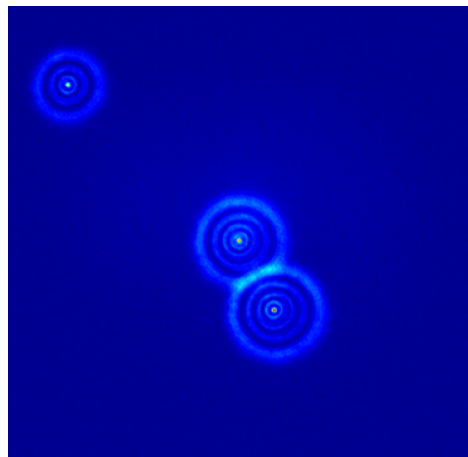


Fig. 9. CCD image of the region for tracking two fixed particles. The two quantum dots in the lower right were selected for the experiment.

The estimated positions of the two particles as well as the photon counts from position one of the measurement constellation are shown in Fig. 10. As with the single fixed particle, the algorithm quickly converged onto the first particle. As seen by the relatively slow rise in the photon counts in Fig. 10(d), the algorithm was slow to converge to the second particle. This was caused primarily by the much larger initial error. Moreover, the choice of $D = 0 \mu\text{m}^2/\text{s}$ in the controller parameters led to a small gain on the error signal in the LQG controller and thus to a slow convergence.

Based on the estimated positions of the two particles, the distance between them can be calculated. The result is shown in Fig. 11.

VI. CONCLUSIONS AND FUTURE WORKS

In this paper we describe experimental results of a system for using a confocal microscope to track multiple fluorescent particles in moving in two-dimensions. The scheme is primarily algorithmic and can therefore be implemented on existing confocal systems with the addition of only a microcontroller or digital signal processor.

As evidenced by the two particle tracking results, the choice of model parameters has a strong influence on the tracking performance. One approach to improving the algorithm, then, is to include online adaptive estimation of model parameters such as diffusion coefficients. This has the additional benefit of providing estimates of biologically-relevant parameters in real time.

Although not directly illustrated by the results reported here, one of the main limits of the tracking speed is the bandwidth of the stage. Based on system identification, the

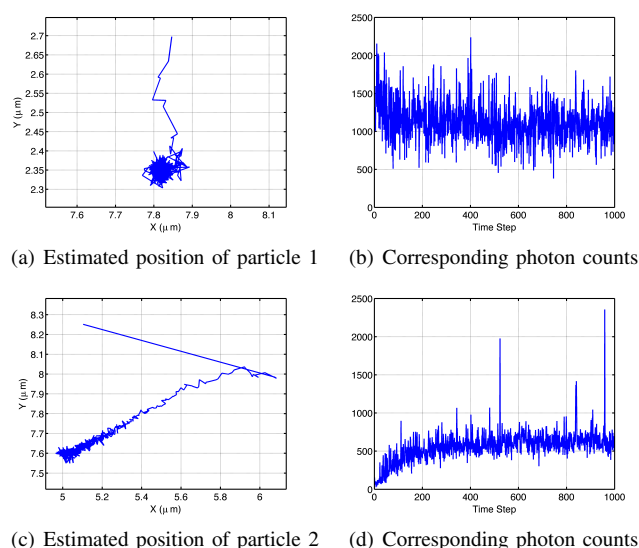


Fig. 10. Tracking two particles. (a) The first particle is fixed to the coverslip while (c) the second is slowly diffusing. The particles were expected to be fixed and so the diffusion coefficient was set to $D = 0 \mu\text{m}^2/\text{s}$. This led to the slow convergence of the algorithm to the particle. This convergence can clearly be seen in the slow rise of the photon counts for particle 2.

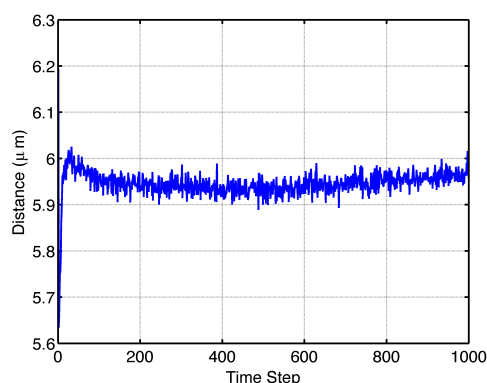


Fig. 11. Estimated distance between the two particles of the tracking experiment in 10.

bandwidth of the piezostage as used in these experiments is between 100-300 Hz, depending on the axis. Simply implementing a more advanced low-level controller for the piezostage can raise this bandwidth significantly, thereby improving the tracking capability. Moreover, the algorithm would work without modification on a confocal microscope that utilized beam steering rather than stage actuation by simply replacing the actuation models. Acousto-optic modulators can achieve beam steering with bandwidths into the MHz range. Tracking would then be limited by intensity level rather than actuator bandwidth.

While the current system focuses on tracking in two dimensions, the extension to three dimensions is relatively straightforward, requiring mainly an extension of the position estimation algorithm into all three dimensions. A theoretical discussion of such an algorithm can be found in [24].

ACKNOWLEDGMENTS

This work supported in part by NSF grant DBI-064983.

REFERENCES

- [1] H. P. Babcock, C. Chen, and X. Zhuang, "Using single-particle tracking to study nuclear trafficking of viral genes," *Biophys. J.*, vol. 87, pp. 2749–2758, 2004.
- [2] T. Fujiwara, K. Ritchie, H. Murakoshi, K. Jacobson, and A. Kusumi, "Phospholipids undergo hop diffusion in compartmentalized cell membrane," *J. Cell Bio.*, vol. 157, no. 6, pp. 1071–1081, 2002.
- [3] F. Daumas, N. Destainville, C. Millot, A. Lopez, D. Dean, and L. Salome, "Confined diffusion without fences of a G-protein-coupled receptor as revealed by single particle tracking," *Biophys. J.*, vol. 84, 2003.
- [4] J. Apgar, Y. Tseng, E. Fedorov, M. B. Herwig, S. C. Almo, and D. Wirtz, "Multiple-particle tracking measurements of heterogeneities in solutions of actin filaments and actin bundles," *Biophys. J.*, vol. 79, 2000.
- [5] M. T. Valentine, P. D. Kaplan, D. Thota, J. C. Crocker, T. Gisler, R. K. Prud'homme, M. Beck, and D. A. Weitz, "Investigating the microenvironments of inhomogeneous soft materials with multiple particle tracking," *Phys. Rev. E*, vol. 64, 2001.
- [6] Y. Tseng, T. P. Kole, and D. Wirtz, "Micromechanical mapping of live cells by multiple-particle-tracking microrheology," *Biophys. J.*, vol. 83, pp. 3162–3176, 2002.
- [7] J. Suh, M. Dawson, and J. Hanes, "Real-time multiple-particle tracking: applications to drug and gene delivery," *Adv. Drug Delivery Rev.*, vol. 57, 2005.
- [8] H. P. Kao and A. S. Verkman, "Tracking of single fluorescent particles in three dimensions: use of cylindrical optics to encode particle position," *Biophys. J.*, vol. 67, pp. 1291–1300, 1994.
- [9] M. Speidel, A. Jonás, and E.-L. Florin, "Three-dimensional tracking of fluorescent nanoparticles with subnanometer precision by use of off-focus imaging," *Opt. Lett.*, vol. 28, no. 2, pp. 69–71, 2003.
- [10] J. Enderlein, "Tracking of fluorescent molecules diffusing within membranes," *Appl. Phys. B*, vol. 71, pp. 773–777, 2000.
- [11] A. J. Berglund and H. Mabuchi, "Feedback controller design for tracking a single fluorescent molecule," *Appl. Phys. B*, vol. 78, 2004.
- [12] V. Levi, Q. Ruan, and E. Gratton, "3-D particle tracking in a two-photon microscope: Application to the study of molecular dynamics in cells," *Biophys. J.*, vol. 88, 2005.
- [13] K. McHale, A. J. Berglund, and H. Mabuchi, "Quantum dot photon statistics measured by three-dimensional particle tracking," *Nano Lett.*, vol. 7, no. 11, pp. 3535–3539, 2007.
- [14] H. Cang, C. M. Wong, C. S. Xu, A. H. Rizvi, and H. Yang, "Confocal three dimensional tracking of a single nanoparticle with concurrent spectroscopic readouts," *Appl. Phys. Lett.*, vol. 88, 2006.
- [15] H. Cang, C. S. Xu, D. Montiel, and H. Yang, "Guiding a confocal microscope by single fluorescent nanoparticles," *Opt. Lett.*, vol. 32, no. 18, pp. 2729–2731, 2007.
- [16] G. A. Lessard, P. M. Goodwin, and J. H. Werner, "Three-dimensional tracking of individual quantum dots," *Appl. Phys. Lett.*, vol. 91, no. 22, p. 224106, 2007.
- [17] W. E. Moerner, "New directions in single-molecule imaging and analysis," *Proc. Nat. Acad. Sci. USA*, vol. 104, no. 31, pp. 12 596–12 602, 2007.
- [18] N. G. Walter, C.-Y. Huang, A. J. Manzo, and M. A. Sobhy, "Do-it-yourself guide how to use the modern single-molecule toolkit," *Nat. Meth.*, vol. 5, no. 6, pp. 475–489, 2008.
- [19] H. Cang, C. S. Xu, and H. Yang, "Progress in single-molecule tracking spectroscopy," *Chem. Phys. Lett.*, vol. 457, pp. 285–291, 2008.
- [20] S. B. Andersson, "Position estimation of fluorescent probes in a confocal microscope," in *Proc. of the IEEE Conf. on Decision and Control*, 2007, pp. 4950–4955.
- [21] —, "Localization of a fluorescent source without numerical fitting," *Opt. Exp.*, vol. 16, no. 23, pp. 18 714–18 724, November 2008.
- [22] Z. Shen and S. B. Andersson, "LQG-based tracking of multiple fluorescent particles in two-dimensions in a confocal microscope," in *Proc. of the American Control Conference*, 2009, pp. 2266–2271.
- [23] J. B. Segur and H. E. Oberstar, "Viscosity of glycerol and its aqueous solutions," *Ind. Eng. Chem.*, vol. 43, no. 9, pp. 2117–2120, 1951.
- [24] T. Sun and S. B. Andersson, "Precise 3-D localization of fluorescent probes without numerical fitting," in *Proc. Engineering in Medicine and Biology Society Conference*, 2007, pp. 4181–4184.